Nonlinear optics of quantum graphs

Rick Lytel, Shoresh Shafei, and Mark G. Kuzyk

Department of Physics and Astronomy, Washington State University, Pullman, Washington 99164-2814

ABSTRACT

Quantum graphs are graphical networks comprised of edges supporting Hamiltonian dynamics and vertices conserving probability flux. Lateral confinement of particle motion on every edge results in a quasi one-dimensional quantum-confined system for which nonlinear optical effects may be calculated. Our ongoing research program is the first to investigate the nonlinear optical properties of quantum graphs. We seek to discover configurations with intrinsic first and second hyperpolarizabilities approaching their respective fundamental limits, to explore the NLO variation with the geometry and topology of the graphs, and to develop scaling laws for more complex graphs with self-similar properties. This paper describes a new methodology for calculating the hyperpolarizabilities of a class of graphs comprised of sequentially-connected edges. Such graphs include closed-loop topologies and their geometrically-similar but topologically-different open loop cousins, as well as other bent wire graphs and their combinations.

Keywords: quantum graphs, hyperpolarizability, fundamental limit, quantum confined systems, quantum wire, nonlinear optical quantum graphs

1. INTRODUCTION

Quantum graphs have emerged as physical models of chaotic dynamical systems over the past two decades.[1,2] Exact solutions for energy spectra have been developed and include closed-form periodic orbit expansions of the spectra for both bare and scaling graphs.[3–7] Nearly all studies of physical quantum graphs treat the electron motion on the graph as tightly confined in the lateral dimension of the edges comprising the graph. As such, these graphs would seem to be candidates for studying the enhancement of nonlinear optical effects in one-dimensional systems due to both confinement and the variety of geometries and topologies available in a graphical network model.

The physics of confinement, and the topological and geometrical properties of the graph are embodied in the transition moments r_{ij}, from which the hyperpolarizability tensors, β_{ijk} (first) and γ_{ijkl} (second) are computed. The transition moments are calculable from the eigenstates and energy spectra of the graph. This work was initiated by our group in 2011,[8] and expanded this year to include loops, stars, and combinations of these.[9] Out of necessity, we invented a new lexicography of quantum states on graphs that enables calculations on arbitrary graphs and describes how to handle unions of solutions on edges to produce eigenstates of graphs and use them in quantum computations for graphs.

The work in this paper describes a new method for computing the nonlinear optical properties of graphs comprised of sequentially-connected edges. This simple formalism is easily applied to bent wires and loops, and should prove most useful for investigations of the mode structure of graphs with hyperpolarizabilities near their fundamental limits.[10] We apply the method to the specific example of a three-sided closed loop to illustrate the way in which the calculations are executed so the methods may gain wide use.

email: rlytel@wsu.edu

Optical Processes in Organic Materials and Nanostructures, edited by Rachel Jakubiak, Manfred Eich, Jean-Michel Nunzi, Proc. of SPIE
Vol. 8474, 84740O · © 2012 SPIE · CCC code: 0277-786/12/$18 · doi: 10.1117/12.928886

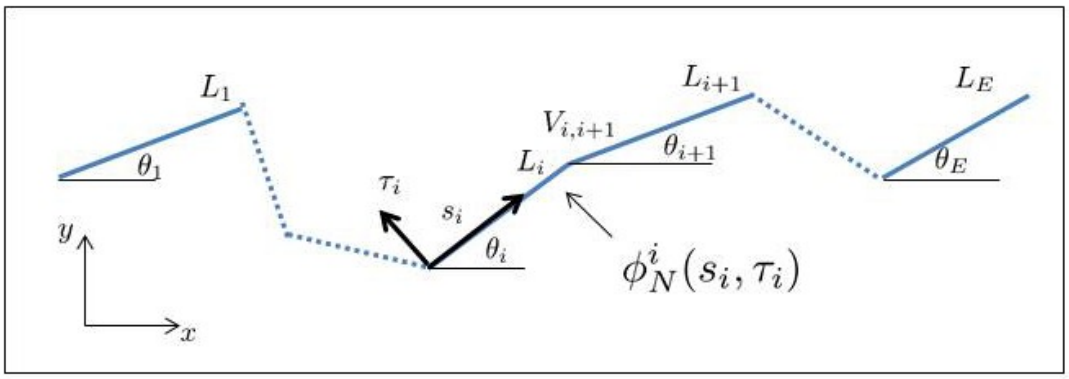

Figure 1. A sequentially-connected quantum graph. Each edge supports wavefunctions that solve the Hamiltonian of the graph with the same eigenvalues. The eigenfunctions of the graph are unions of the edge states, $\phi_n^i(s_i, \tau_i)$.

2. NONLINEAR OPTICS OF QUANTUM GRAPHS

A quantum graph is comprised of edges (wires), each of which supports particle dynamics governed by the same Hamiltonian. The graph has a set of eigenstates and an energy spectrum that is also the spectrum of eigenvalues of the Hamiltonian on each edge. Edge solutions are not a complete set of eigenstates of the Hamiltonian, however, as they are matched at the vertices of the graph to edge states from other edges to maintain continuity and flux conservation at vertices. The union of the wavefunctions on each edge of the graph is an eigenstate, however, because the value of the wavefunction of the particle on any specific edge is exactly equal to the union evaluated on that edge. Figure 1 illustrates the sequentially-connected graphs that are the subjects of this paper.

The nonlinear optical properties of the graph are determined by the hyperpolarizabity tensors. These may be calculated from the transition moments, which are in turn calculated using the eigenstates and energy spectra. The symmetries of the graph control the geometric and topological features of the hyperpolarizabilites. Here, we describe a general method to solve for the hyperpolarizabilities of these graphs. We use a single-electron model, off-resonance, and confine its motion to the longitudinal direction s along the wires.[8,10]

2.1 Matrix elements for sequentially-connected quantum graphs

We introduce a general method for computing the transition moments of a graph with E edges using a set of eigenstates $\psi_n(s)$, where s is measured along the graph from a convenient origin, the lengths of the edges of the graph are L_p, and the angles each edge makes with an x-axis in the lab are denoted by θ_p.

The eigenfunctions $\psi_n(s)$ are unions over the graph of the edge functions $\phi_n^i(s_i)$ in the sense that they are equal to the edge functions on edge i when the particle is considered to be on that edge. Since the edge functions are matched in magnitude and flux at the vertices, the particle on the graph in Fig 1 doesn't know anything about edges (as we assume the transitions from one edge to the next are continuous at the vertices). From its viewpoint, its dynamics is described a continuous wavefunction, the eigenfunction of the graph. To illustrate how to exploit this observation, write x_{nm} as a sum of the moments calculated on each edge, using the value of the x-projection on the specific edge, accumulated from the origin:

$$x_{nm} = \sum_{k=1}^{E} \int_k ds_k \; x(s_k) \phi_n^{*k}(s_k) \phi_m^k(s_k) \tag{1}$$

where the sum is a real sum, not a union, of the integrals taken on each edge of the value of x on that edge times the product of the two wavefunctions on that edge. Since the graph is sequentially-connected, each integral in

Eqn (1) begins at a lower limit where the previous integral has its upper limit. Consequently, we may leverage this feature by writing the transition moments in terms of the value of the eigenfunction on that edge using a continuous integral:

$$x_{nm} = \int_0^R ds\ x(s)\psi_m^*(s)\psi_n(s) \tag{2}$$

where R is the total length and $x(s)$ is the x-position of the particle as it moves through the loop. The value of $x(s)$ to be used in this equation is given by its value at each location spanned by the integral. We may write this as

$$x(s) = \sum_{p=1}^{k-1} L_p \cos\theta_p + \left(s - \sum_{p=1}^{k-1} L_p \right) \cos\theta_k. \tag{3}$$

where again we emphasize that this expression has meaning in Eqn (2) when its index k is the same as the interval in the integrand that spans the kth segment. The transition moments are then given as

$$\begin{aligned} x_{nm} &= \sum_{k=1}^{E} \cos\theta_k J_{nm}(a_k, b_k) \\ &+ \sum_{k=2}^{E} \left(\sum_{p=1}^{k-1} L_p \left(\cos\theta_p - \cos\theta_k \right) \right) I_{nm}(a_k, b_k) \end{aligned} \tag{4}$$

where

$$a_k = \sum_{p=1}^{k-1} L_p,\ \ b_k = \sum_{p=1}^{k} L_p \tag{5}$$

and the mode overlap integrals are

$$\begin{aligned} I_{nm}(a,b) &= \int_a^b ds\ \psi_m^*(s)\psi_n(s) \\ J_{nm}(a,b) &= \int_a^b s\ ds\ \psi_m^*(s)\psi_n(s). \end{aligned} \tag{6}$$

The formulation in Eqn (4) clearly shows that the geometry of the quantum graph controls the x_{nm} through the angular factors describing the graph, while the characteristics of the graph that set the boundary conditions and thus determine the eigenstates control the x_{nm} through the integrals in Eqn (6). For a given graph, the angles are fixed but the basis states may be any specific set of orthonormal states that solve the graph. The result will be that the x_{nm} are basis-state dependent. However, the physical quantities are invariant to a change of basis states.

A convenient feature of this approach is that it is straightforward to compute the matrix elements y_{nm}, which are defined as

$$y_{nm} = \int_0^R ds\ y(s)\psi_m^*(s)\psi_n(s) \tag{7}$$

where $y(s)$ is obtained from Eqn. 4 by replacing $\cos\theta_p$ with $\sin\theta_p$. This leads to an expression for y_{nm} that is identical in form to Eqn. (4) but with the sine of the angles instead of the cosine.

To sum up, the graph is specified by its vertices and the Hamiltonian operating on the edges connecting the vertices in a prescribed way. For a sequentially-connected graph, the edges are joined end-to-end. The edge wavefunctions may be found up to a multiplicative complex constant by solving the appropriate wave equation. Continuity and flux conservation at the vertices produces a union of edges which may be written as a single,

continuous function of s, subject to the proper interpretation of what it means to be on an edge k. For a general graph, the matrix of equations relating edge amplitudes has a nontrivial solution for energies satisfying the secular equation of the matrix. For sequential graphs, the energy spectrum is easier to obtain and follows from the specific boundary conditions imposed at the ends of the graph. For loops, the wavefunction must repeat after each loop, so the wave numbers are $2\pi n/R$, with $n = 0, \pm 1, \pm 2....$ For terminal ends, the potential is assigned an infinite value, and the wavefunction must vanish. This sets the energy spectrum at positive integer multiples of π/R. Other potentials may be selected to generate interesting boundary conditions and spectra. The eigenstates of the graph, expressed as a union of edge states calculated in this way are orthogonal and may be normalized in the usual way. The graph is considered solved when the eigenstates and energies are in hand.

2.2 Hyperpolarizability tensors

The nonlinear optical properties of the quantum graph system are described by the first and second hyperpolarizability tensors β_{ijk} and γ_{ijkl}, and are a sum over states (SOS) of products of the transition moments of the graph. We work with tensors normalized to their maximum allowable values from the theory of fundamental limits.[10] These are:

$$\begin{aligned} \beta_{max} &= 3^{1/4}\left(\frac{e\hbar}{\sqrt{m}}\right)^3\left(\frac{N^{3/2}}{E_{10}^{7/2}}\right) \\ \gamma_{max} &= 4\left(\frac{e\hbar}{\sqrt{m}}\right)^4\left(\frac{N^2}{E_{10}^5}\right) \end{aligned} \tag{8}$$

Normalizing the hyperpolarizability this way ensures that the size of the system is scaled out of the calculation, making it simple to compare results among different graphs based solely on shape and configuration.

For this investigation, we need the off-resonance expressions for the hyperpolarizability tensors, which are provided in many sources, eg, Ref.[10]

$$\beta_{ijk} = -.5e^3 P_{ijk}{\sum_{n,m}}' \frac{r_{0n}^i \bar{r}_{nm}^j r_{m0}^k}{E_{n0}E_{m0}}, \tag{9}$$

where the sum is over all modes except for the ground state, and $\bar{r}_{nm} \equiv r_{nm} - r_{00}\delta_{nm}$, and P_{ijk} permutes all the indices in the expression. The SOS expression for γ_{int} is

$$\gamma_{ijkl} = (1/6)P_{ijkl}\left({\sum_{n,m,l}}' \frac{r_{0n}^i \bar{r}_{nm}^j \bar{r}_{ml}^k r_{l0}^l}{E_{n0}E_{m0}E_{l0}} - {\sum_{n,m}}' \frac{r_{0n}^i r_{n0}^j r_{0m}^k r_{m0}^l}{E_{n0}^2 E_{m0}}\right) \tag{10}$$

where the permutation operator again permutes all indices.

For both of these expressions, the transition moments r_{ij} are computed in an appropriate orthonormal basis set for the graph, with the integrations taken along the path of the graph with $r(s)$ defined by the (cumulative) projection of s onto the $x-axis$ (r=x) or the $y-axis$ (r=y). Eqn (4) allows direct calculation of x_{nm} and y_{nm}, and consequently, the hyperpolarizabilities may be directly computed by Eqns (9) and (10).

Far from resonance, the hyperpolarizability tensor β_{ijk} is a fully symmetric, third rank tensor with four independent Cartesian components. Similarly, γ_{ijkl} is a fully symmetric, fourth rank tensor and has five independent Cartesian components.[11] We will refer to the independent components for β as the set $(\beta_{xxx}, \beta_{xxy}, \beta_{xyy}, \beta_{yyy})$ and for γ the set $(\gamma_{xxxx}, \gamma_{xxxy}, \gamma_{xxyy}, \gamma_{xyyy}, \gamma_{yyyy})$ where the components are measured in some specified reference frame and are related to those in another frame by a suitable transformation of the hyperpolarizability tensors. The determination of the NLO properties of the graph is thus reduced to the calculation of the tensors for graphs with a specific geometry for which states and spectra are known.

It is common practice to refer to β_{xxx} by its largest value in the lab when the molecule (graph) has been rotated to the optimum position. To find this position, we specify the graph, calculate the four nonzero components of β_{ijk}, and note that the value of β_{xxx} in the lab when the graph has been rotated through an angle θ is given by

$$\beta_{xxx}(\theta) = \beta_{xxx}\cos^3\theta + 3\beta_{xxy}\cos^2\theta\sin\theta + 3\beta_{xyy}\cos\theta\sin^2\theta + \beta_{yyy}\sin^3\theta \tag{11}$$

where the tensor components are directly calculable from their sum over states expansions using both x_{ij} and y_{ij}. The angle which maximizes the left hand side of Eqn (11 is then easily found. Similar remarks hold for γ, with the expansion in the lab frame given by

$$\gamma_{xxxx}(\theta) = \gamma_{xxxx}\cos^4\theta + 4\gamma_{xxxy}\cos^3\theta\sin\theta + 6\gamma_{xxyy}\cos^2\theta\sin^2\theta + 4\gamma_{xyyy}\cos\theta\sin^3\theta + \gamma_{yyyy}\sin^4\theta \tag{12}$$

Though out of scope for the investigations in this paper, we note that a spherical tensor approach generally provides the clearest understanding of the impact of symmetry on the nonlinear optical properties. Zyss et.al[12] and Joffre et. al[13] discuss the molecular nonlinearities in multipolar media using irreducible, spherical representations for β, an approach which provides insight into the shape-dependence of the first hyperpolarizability, particularly with respect to certain symmetry groups. The transformation from a Cartesian to a spherical tensor representation is straightforward[14] and is explored elsewhere for nonlinear optical graphs.[9]

We do wish to display the tensor norms, defined by

$$\beta_{rms} = \sqrt{\left(\beta_{xxx}^2 + 3\beta_{xxy}^2 + 3\beta_{xyy}^2 + \beta_{yyy}^2\right)} \tag{13}$$

and

$$\gamma_{rms} = \sqrt{\left(\gamma_{xxxx}^2 + 4\gamma_{xxxy}^2 + 6\gamma_{xxyy}^2 + 4\gamma_{xyyy} + \gamma_{yyyy}^2\right)} \tag{14}$$

as these are invariant under all rotation group transformations of the hyperpolarizability tensors.

To summarize, we have shown how to use the transition moments x_{ij} and y_{ij} for a solved quantum graph to calculate the first and second hyperpolarizability of the graph in order to determine the effect of shape and topology on their magnitudes.[9] This approach provides guidance to both molecular designers of nonlinear optical quantum-confined systems and to theorists seeking to discover structures with nonlinearities approaching the fundamental limit.

3. QUANTUM LOOP EXAMPLES

We apply the computational method described in the previous sections to determine the hyperpolarizabilities of $E = 3$ closed loop (triangle) graphs. The method is nearly identical to that required to solve the open loop versions of the triangle graphs. It is worth noting that opening a vertex of a triangle graph even slightly dramatically changes the states and energy spectra, even if the overall shape remains identical to the closed-loop triangle. Bent wires that are wide open are substantially different than the partially closed ones, due to geometrical effects. These are explored elsewhere.[9]

The edge wavefunctions $\phi_n^k(s)$ may be written as solutions to the free-particle Schrodinger equation. For a sequentially-connected graph, continuity at the vertices is guaranteed of the wavefunctions accumulate a path-dependent phase from one edge to the next, as previously illustrated. This means that we may construct integrals of matrix elements of the graph as a quasi- continuous integral over s of a single function whose value on a specific edge is that of the edge wavefunction when the particle is on that edge. A closed loop necessarily has wave numbers $k_n = 2\pi n/R$ with $n = 0, \pm1, \pm2, ...$ in order to ensure that the physics is the same no matter how many times the particle might traverse the closed loop. A simple set of eigenstates for the loop are the counterpropagating traveling-wave eigenstates:

$$\psi_n^{TW}(s) = 1/\sqrt{R}\exp(ik_n s), \tag{15}$$

for all modes n. The ground state is a singlet with zero energy and a constant wavefunction. All other states are doubly degenerate. We emphasize again that Eqn (15) must be interpreted as an eigenfunction of the graph whose value on an edge is equal to that edge's wavefunction. With that in mind, we may freely work with the eigenfunctions and explore standing wave and even mode-dependent combination states in order to investigate the importance of specific states to the hyperpolarizabilities.

For example, we may construct a complete, orthonormal set of standing wave states as

$$\psi_n^{SW}(s) = \sqrt{2/R}\sin(k_n s + \phi) \tag{16}$$

where ϕ is a mixing angle for the circular function solutions to the free-particle wave equation. It is straightforward to show that these states may be obtained from the free-particle states if $\phi = \pi/4$. This choice ensures that the new basis is orthonormal.

An even richer family of mixed basis states is easily generated from the free-particle basis by superposing degenerate modes with an arbitrary admixture component, δ_n as follows:

$$\psi_n^{MX}(s) = \frac{\psi_n^{TW}(s) + i\delta_n \psi_{-n}^{TW}(s)}{\sqrt{(1+\delta_n^2}} \tag{17}$$

It is straightforward to show that these states are orthonormal if $\delta_n = \delta_{-n}$. The transition moments x_{nm} in this basis may be expressed in terms of those for the TW basis for arbitrary δ_n. The results in this family of basis sets are identical to those in any other basis set. But the choice of δ_n allows one to 'pick' the most important transitions for the nonlinear process on a mode-by-mode basis.

All of these states give equivalent results for the hyperpolarizabilities, as well in sum rules,[8,15,16] despite each set leading to different transition moments. For the triangle loops, Eqn. (2) for the transition moments with basis states on the loop given by $\psi_n(s)$ becomes

$$\begin{aligned} x_{nm} &= \int_0^{L_1} ds\ x_1 D_{nm}(s) \\ &+ \int_{L_1}^{L_1+L_2} ds\ x_2 D_{nm}(s) \\ &+ \int_{L_1+L_2}^{L_1+L_2+L_3} ds\ x_3 D_{nm}(s) \end{aligned} \tag{18}$$

where $D_{nm} \equiv \psi_m^*(s)\psi_n(s)$ and the x_i are given by

$$\begin{aligned} x_1 &= s\cos\theta_1, \\ x_2 &= L_1\cos\theta_1 + (s-L_1)\cos\theta_2 \\ x_3 &= L_1\cos\theta_1 + L_2\cos\theta_2 + (s-L_1-L_2)\cos\theta_3 \end{aligned} \tag{19}$$

Eqns. (18) and (19) combine to give the three-segment version of Eqn. (4):

$$\begin{aligned} x_{nm} &= \cos\theta_1 J_{nm}(0, L_1) + \cos\theta_2 J_{nm}(L_1, L_1+L_2) \\ &+ \cos\theta_3 J_{nm}(L_1+L_2, L_1+L_2+L_3) \\ &+ L_1(\cos\theta_1 - \cos\theta_2) I_{nm}(L_1, L_1+L_2) \\ &+ [L_1(\cos\theta_1 - \cos\theta_3) + L_2(\cos\theta_2 - \cos\theta_3)] \\ &\times I_{nm}(L_1+L_2, L_1+L_2+L_3) \end{aligned} \tag{20}$$

The loop can be fully characterized by its three vertices, as these determine the angles θ_i each segment makes with the x-axis.

At this point, we wish to emphasize that the expression in Eqn (20) applies to this graph even if a vertex is opened, provided that the new eigenstates and energies are used to compute the mode overlap integrals. A geometric clone of the closed loop graph but with one vertex open has the same angular dependence as the closed-loop graph, but the different states and spectra result in a radically different set of hyperpolarizabilities.[9] Topology, not geometry, appears to have the largest effect on the nonlinear optical responses of the graphs.

Returning to the calculation, once the eigenstates are selected, the mode overlap integrals are easily calculated from Eqn (6) as

$$\begin{aligned} I_{nm}(a,b) &= \int_a^b ds D_{nm}(s) \\ J_{nm}(a,b) &= \int_a^b s ds D_{nm}(s) \end{aligned} \tag{21}$$

It is now straightforward to calculate the mode overlap integrals for the three sets of eigenstates displayed in Eqns. (15), (16), and (17). For the traveling-wave eigenstates given in Eqn. (15), the product D_{nm} in the integrands of Eqn. (21) may be written as

$$D_{nm} = (1/R)\exp(\imath k^-_{nm}(s)) \tag{22}$$

Here, we define $k^{\pm}_{nm} = k_n \pm k_m$. The mode overlap integrals are then given by

$$I_{nm}(a,b) = \left(1/\imath k^-_{nm}\right)\left[\exp(\imath k^-_{nm} b) - \exp(\imath k^-_{nm} a)\right] \tag{23}$$

and

$$\begin{aligned} J_{nm}(a,b) &= \left(1/\imath k^-_{nm}\right)\left[b\exp(\imath k^-_{nm} b) - a\exp(\imath k^-_{nm} a)\right] \\ &- \left(1/\imath k^-_{nm}\right) I_{nm}(a,b) \end{aligned} \tag{24}$$

For the standing-wave eigenstates given in Eqn. (16) with $\phi = \pi/4$, D_{nm} may be written as

$$D_{nm} = (1/R)\left[\cos k^-_{nm} s + \sin k^+_{nm} s\right] \tag{25}$$

The mode overlap integrals are then given by

$$\begin{aligned} I_{nm}(a,b) &= \left[b sinc(k^-_{nm} b) - a sinc(k^-_{nm} a)\right] \\ &- \left[\cos k^-_{nm} b - \cos k^+_{nm} a\right]/k^+_{nm} \end{aligned} \tag{26}$$

$$\begin{aligned} J_{nm}(a,b) &= \left[b^2 sinc(k^-_{nm} b) - a^2 sinc(k^-_{nm} a)\right] \\ &- .5\left[b^2 sinc^2(k^-_{nm} b/2) - a^2 sinc^2(k^-_{nm} a/2)\right] \\ &+ \left[a\cos k^+_{nm} a - b\cos k^+_{nm} b\right]/k^+_{nm} \\ &+ \left[\sin k^+_{nm} b - \sin k^+_{nm} a\right]/(k^+_{nm})^2 \end{aligned} \tag{27}$$

where $sinc(x) \equiv \sin(x)/x$. Finally, for the mixed states in Eqn. (17), the transition moments may be expressed in terms of those for the pure traveling-wave states, viz,

$$x^{mixed}_{nm} = \frac{\left[x^{TW}_{nm} + \delta_n\delta_m x^{TW}_{-n-m} + \imath\left(\delta_m x^{TW}_{n-m} - \delta_n x^{TW}_{-nm}\right)\right]}{\sqrt{1+\delta_n^2}\sqrt{1+\delta_m^2}} \tag{28}$$

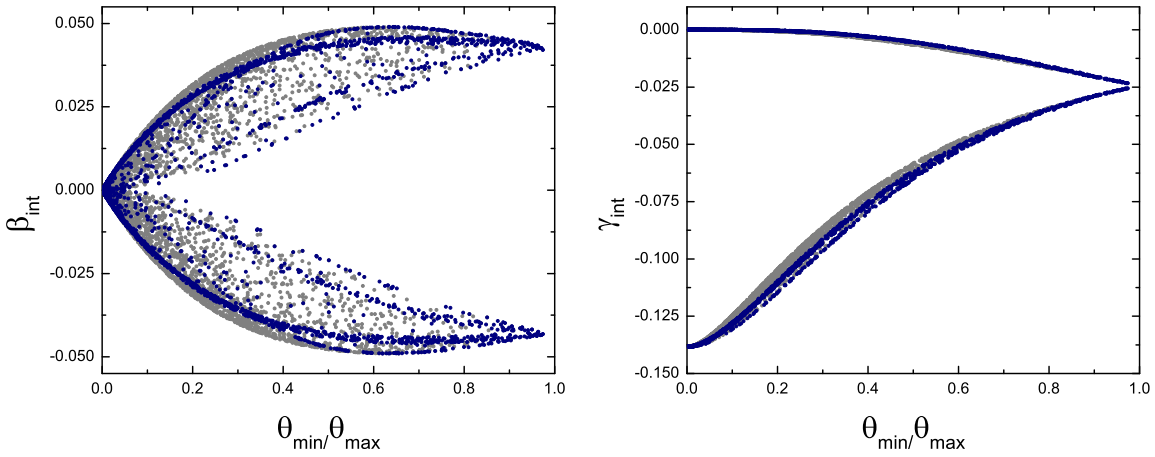

Figure 2. β_{int} and γ_{int} as functions of the aspect ratio of the triangle loops. The dark blue points are the isosceles-like triangles.

The calculation of the hyperpolarizabilities using the mixed states in Eqn. (17) yields identical results to those found in the counterpropagating and standing-wave eigenstates. However, one can tune the way the degenerate modes mix to control how much of one over the other contributes to the transition moments. Note that the relationship between β and the normalized dipole moment $X = |x_{10}|/|x_{10}|^{max}$, a metric for NLO response,[17] is basis-independent as long as the matrix element in X takes the form of a linear combination of the mixed states $\left(|y_{10}|^2 + |y_{-10}|^2\right)$ where

$$\begin{aligned} y_{10} &= (x_{10} - \imath\delta_n x_{-10}) \\ y_{01} &= (x_{01} + \imath\delta_n x_{0-1}) \\ y_{-10} &= (x_{-10} - \imath\delta_n x_{10}) \\ y_{0-1} &= (x_{0-1} + \imath\delta_n x_{01}) \end{aligned} \tag{29}$$

Figure 2 displays the magnitude of the intrinsic diagonal x components of the first hyperpolarizability (left) and second hyperpolarizability (right) as a function of the aspect ratio of the triangle loops. The magnitude and signs of these have been discussed elsewhere.[9,15] We note for completeness that the second hyperpolarizability is always negative for a closed loop. Interestingly, opening a vertex increases the maximum β_{int} by a factor of about three while enabling positive γ_{int} for a range of triangles.[15] For our purposes here, we emphasize that these calculations were accomplished with each of the three sets of eigenstates described here, and as expected, identical results were obtained for each. Future studies will discuss the variation in the modes when basis sets are changed. The methods displayed in this paper should encourage the study of such variations by interested researchers.

4. CONCLUSIONS

This paper presented a complete method for computing the hyperpolarizabilities of sequentially-connected quantum graphs that is easily applied to any desired set of basis states and for any graph geometry or topology, so long as the integration along the graph's path from start to finish is continuous. It may be extended to graphs with branches with a little care.

ACKNOWLEDGMENTS

S. Shafei and M. G. Kuzyk would like to thank the National Science Foundation (NSF) (ECCS-1128076) for generously supporting this work.

REFERENCES

[1] T. Kottos and U. Smilansky, "Quantum chaos on graphs," *Phys. Rev. Lett.* **79**, pp. 4794–4797, Dec 1997.

[2] T. Kottos and U. Smilansky, "Periodic orbit theory and spectral statistics for quantum graphs," *Ann. Phys.* **274**(1), pp. 76–124, 1999.

[3] Y. Dabaghian and R. Blümel, "Explicit spectral formulas for scaling quantum graphs," *Phys. Rev. E* **70**, p. 046206, Oct 2004.

[4] Y. Dabaghian and R. Blümel, "Explicit analytical solution for scaling quantum graphs," *Phys. Rev. E* **68**, p. 055201, Nov 2003.

[5] Y. Dabaghian, R. Jensen, and R. Blmel, "Spectra of regular quantum graphs," *Journal of Experimental and Theoretical Physics* **94**, pp. 1201–1215, 2002. 10.1134/1.1493174.

[6] R. Blümel, Y. Dabaghian, and R. V. Jensen, "Explicitly solvable cases of one-dimensional quantum chaos," *Phys. Rev. Lett.* **88**, p. 044101, Jan 2002.

[7] R. Blümel, Y. Dabaghian, and R. V. Jensen, "Exact, convergent periodic-orbit expansions of individual energy eigenvalues of regular quantum graphs," *Phys. Rev. E* **65**, p. 046222, Apr 2002.

[8] S. Shafei and M. G. Kuzyk, "The effect of extreme confinement on the nonlinear-optical response of quantum wires," *J. Nonl. Opt. Phys. Mat.* **20**, pp. 427–441, 2011.

[9] R. Lytel, S. Shafei, J. H. Smith, and M. G. Kuzyk, "The influence of geometry and topology of quantum graphs on their nonlinear-optical properties," *ArXiv e-prints* , July 2012.

[10] M. G. Kuzyk, "Physical Limits on Electronic Nonlinear Molecular Susceptibilities," *Phys. Rev. Lett.* **85**, p. 1218, 2000.

[11] T. Bancewicz and Z. Ożgo, "Irreducible spherical representation of some fourth-rank tensors," *J. Comput. Meth. Sci. Eng.* **10**(3), pp. 129–138, 2010.

[12] J. Zyss and I. Ledoux, "Nonlinear optics in multipolar media: theory and experiments," *Chem. Rev.* **94**(1), pp. 77–105, 1994.

[13] M. Joffre, D. Yaron, J. Silbey, and J. Zyss, "Second Order Optical Nonlinearity in Octupolar Aromatic Systems," *J . Chem. Phys.* **97**(8), pp. 5607–5615, 1992.

[14] J. Jerphagnon, D. Chemla, and R. Bonneville, "The description of the physical properties of condensed matter using irreducible tensors," *Adv. Phys.* **27**(4), pp. 609–650, 1978.

[15] S. Shafei, R. Lytel, and M. G. Kuzyk, "Geometry-controlled nonlinear optical response of quantum graphs," *ArXiv e-prints* , Aug. 2012.

[16] S. Wang, "Generalization of the thomas-reiche-kuhn and the bethe sum rules," *Phys. Rev. A* **60**(1), pp. 262–266, 1999.

[17] S. Shafei and M. G. Kuzyk, "Critical role of the energy spectrum in determining the nonlinear-optical response of a quantum system," *J. Opt. Soc. Am. B* **28**, pp. 882–891, 2011.